



Gold clusters supported on alkaline treated TS-1 for highly efficient propene epoxidation with O₂ and H₂

Jiahui Huang ^{a,c}, Takashi Takei ^{a,c}, Tomoki Akita ^{b,c}, Hironori Ohashi ^{a,c}, Masatake Haruta ^{a,c,*}

^a Graduate School of Urban Environmental Sciences, Tokyo Metropolitan University, 1-1 Minami-osawa, Hachioji, Tokyo 192-0397, Japan

^b Research Institute for Ubiquitous Energy Devices, National Institute of Advanced Industrial Science and Technology (AIST), 1-8-31 Midorigaoka, Ikeda, Osaka 563-8577, Japan

^c Japan Science and Technology Agency (JST), CREST, 4-1-8 Hon-cho, Kawaguchi, Saitama 332-0012, Japan

ARTICLE INFO

Article history:

Received 11 November 2009
Received in revised form 19 January 2010
Accepted 20 January 2010
Available online 25 January 2010

Keywords:

Propene epoxidation
O₂/H₂ mixture
TS-1
Alkaline treatment
Gold cluster
H₂ efficiency

ABSTRACT

Gold could be deposited as clusters smaller than 2.0 nm in diameter on TS-1 by solid grinding (SG) of the support with dimethyl Au(III) acetylacetone after TS-1 was pretreated in aqueous solution of alkaline metal hydroxides. While in C₃H₆ epoxidation with O₂ and H₂ mixture Au nanoparticles larger than 2.0 nm deposited on TS-1 without alkaline treatment gave a very low PO formation rate of 11 gPO kg_{cat.}⁻¹ h⁻¹, Au clusters on alkaline treated TS-1 presented a greatly enhanced rate as high as 137 gPO kg_{cat.}⁻¹ h⁻¹, which was comparable to the best data reported so far. In addition, very high H₂ efficiency reaching 47% could be obtained by gold clusters on alkaline treated TS-1.

© 2010 Elsevier B.V. All rights reserved.

1. Introduction

Propene epoxide (PO) is an important bulk chemical and mainly used to produce polyurethane foams and resins, and propylene glycol. Its annual worldwide production was about 7.5 million tons with a growth rate above 4.0% in 2007 [1]. PO is currently mainly produced by the chlorohydrin process and several organic peroxide processes [2]. The former is accompanied by the by-production of CaCl₂ together with toxic chlorinated organic compounds. The latter suffers from the mismatch of market demand between PO and co-products such as tert-butanol and styrene. Recently two new processes have been developed: a cumene hydroperoxide process in 2003 in Japan [3] and a hydrogen peroxide (H₂O₂) epoxidation process in 2008 in Belgium [4]. The cumene hydroperoxide process produces PO alone by reducing co-product, cumyl alcohol, to cumene with H₂. The H₂O₂ epoxidation process produces H₂O as the only by-product, while H₂O₂ is usually expensive and its commercial production requires two steps: anthraquinone hydrogenation and subsequent oxida-

tion [5]. Accordingly, the common constraint of these new industrial processes is multi-staged reactions in liquid phase.

Our research group firstly reported in 1998 that gold (Au) nanoparticles (NPs, 2.0–5.0 nm) deposited on anatase TiO₂ could catalyze gas phase propene (C₃H₆) epoxidation with O₂ and H₂ mixture to produce PO with selectivity above 90% [6]. In contrast to commercial processes described above for PO synthesis, this route is simpler (one-step reaction in gas phase) and greener (with H₂O as the only by-product), and thus soon has attracted growing interests.

In the past decade anatase TiO₂, mesoporous Ti-silicate (Ti-SiO₂), and microporous titanosilicalite-1 (TS-1) have been extensively used as supports for Au catalysts for C₃H₆ epoxidation with O₂ and H₂ mixture under hourly space velocity of 4000–8000 mL g_{cat.}⁻¹ h⁻¹ [6–21]. When Au NPs were supported on anatase TiO₂, they were selective to PO only at temperatures below 373 K, therefore giving C₃H₆ conversions less than 1.0% [6,13]. However, if Au NPs were loaded on the latter two supports, they were selective up to 473 K exhibiting higher catalytic performance [7,8,12,17–20]. In the presence of solid promoter Ba(NO₃)₂ on the catalyst and gas phase promoter trimethylamine in the reactant feed gas, 0.30 wt% Au/mesoporous Ti-SiO₂ displayed a C₃H₆ conversion of 8.5% at a PO selectivity of 91% and at a H₂ efficiency of about 35% at 423 K [8], whereas 0.05 wt% Au/TS-1(Si/Ti = 36) showed without promoters a C₃H₆ conversion of 8.8% at a PO selectivity of 81% at 473 K (H₂ efficiency has not been given),

* Corresponding author. Present address: Department of Applied Chemistry, Graduate School of Urban Environmental Sciences, Tokyo Metropolitan University, 1-1 Minami-osawa, Hachioji, Tokyo 192-0397, Japan. Tel.: +81 42 677 2851; fax: +81 42 677 2852.

E-mail address: haruta-masatake@center.tmu.ac.jp (M. Haruta).

corresponding to a PO formation rate of $116 \text{ g}_{\text{PO}} \text{ kg}_{\text{cat.}}^{-1} \text{ h}^{-1}$ [18]. The PO formation rate over Au/TS-1 has been improved to $134 \text{ g}_{\text{PO}} \text{ kg}_{\text{cat.}}^{-1} \text{ h}^{-1}$ by pretreating TS-1 with NH_4NO_3 aqueous solution before Au deposition by deposition-precipitation (DP) [19] and to $132 \text{ g}_{\text{PO}} \text{ kg}_{\text{cat.}}^{-1} \text{ h}^{-1}$ by adding carbon pearls to the sol-gel during the synthesis of TS-1 support [20]. Recently, PO formation rate over Au/TS-1 was further improved to $200 \text{ g}_{\text{PO}} \text{ kg}_{\text{cat.}}^{-1} \text{ h}^{-1}$ by using a packed-bed catalytic membrane reactor, in which concentrations of O_2 and H_2 could be increased to 40% each [12].

Although DP method is very effective to prepare highly active Au/TS-1 for C_3H_6 epoxidation with O_2 and H_2 mixture [12,17–21], the capture efficiency of Au was always very low because of the hydrophobic nature of TS-1. Even though TS-1 support was pretreated with NH_4NO_3 aqueous solution before DP [19] or a certain amount of alkaline earth metal nitrates was added to the suspension of TS-1 in HAuCl_4 solution during DP [21], the capture efficiency of Au was still less than 20%. Recently we have reported that solid grinding (SG) of the support materials with dimethyl Au(III) acetylacetone can deposit small Au NPs and/or clusters on organic polymers, carbons, and base metal oxides with very high Au capture efficiency (86–100%) [22,23].

Here SG method was used to deposit Au on as prepared TS-1 and alkaline treated TS-1 with very high Au capture efficiency of about 100%. In C_3H_6 epoxidation with O_2 and H_2 mixture Au/TS-1 showed a very low C_3H_6 conversion of 0.6%, while Au/alkaline treated TS-1 yielded greatly improved C_3H_6 conversions. Over 0.25 wt% Au/TS-1-Na1 (see Section 2 for the preparation of TS-1-Na1) a high C_3H_6 conversion of 8.8% was achieved with PO selectivity of 82%, resulting in a high PO formation rate of $137 \text{ g}_{\text{PO}} \text{ kg}_{\text{cat.}}^{-1} \text{ h}^{-1}$, comparable to the best results reported by Delgass and co-workers [19,20]. In addition, a very high H_2 utilization efficiency of 47%, better than any other reported one in published publications, was achieved over Au/TS-1-Na1 with a low Au loading of 0.05 wt%. Further characterizations strongly suggest that the presence of a large number of Au clusters (1.0–2.0 nm) over the exterior surface of Au/alkaline treated TS-1 are responsible for the greatly enhanced catalytic performance.

2. Experimental

2.1. Preparation of TS-1

Tetrapropylammonium hydroxide (TPAOH, 25 wt%), 25.2 g, was dissolved in 48.0 g of H_2O . To this solution a mixture of tetraethyl orthosilicate (21.0 g) and the required amount of tetrabutyl orthotitanate was, after stirring for 0.5 h, added dropwise under vigorous stirring at room temperature. After further stirring for 12 h at room temperature, 12.0 g of poly(acrylamide-co-diallyldimethylammonium chloride) (10 wt% in water) was added. The resulting mixture was further stirred vigorously for 24 h at room temperature, transferred to a teflon-lined stainless autoclave, and then hydrothermally treated at 453 K for 120 h. Products were dried at 383 K for 24 h, and then calcined in air at 823 K for 5.0 h. The TS-1 obtained was named as TS-1(x), where x is the molar ratio of silicon (Si) to titanium (Ti).

2.2. Pretreatment of TS-1 in aqueous alkaline solution

To the suspension of 1.0 g of calcined TS-1 in 100 mL H_2O , a 1.0 M aqueous solution of NaOH , LiOH , KOH or CsOH was added dropwise under vigorous stirring at 303 K until the pH reached 12. The pH was kept at this value for the required period by dropping a small amount of aqueous alkaline metal hydroxide solution. The suspension was collected by filtration, washed 5 times with 2000 mL (total amount) of H_2O to remove residual alkaline metal

hydroxide and then dried at 373 K overnight in air. The alkaline treated TS-1 was named as TS-1(x)-My, where M (M = Li, Na, K or Cs) stands for alkaline metal hydroxide and y stands for $y(\text{h})$ of alkaline treatment period.

2.3. Deposition of Au by SG

Solid grinding was used to deposit Au on as prepared TS-1 and alkaline treated TS-1 [22,23]. The powder of the supports and the required amount of dimethyl Au(III) acetylacetone [$(\text{CH}_3)_2\text{Au}(\text{acac})$] having a vapor pressure of 1.1 Pa at 298 K were ground in an agate mortar in air for 15 min at room temperature, followed by reduction in a stream (20 mL min^{-1}) of 10 vol% H_2 in Ar at 423 K for 1.0 h. The temperature was raised from room temperature to 423 K at a heating rate of 1.0 K min^{-1} . The Au catalysts thus prepared were denoted as z -Au/TS-1(x)-My, where z is the calculated weight percent of Au in the catalysts. Because dimethyl Au(III) acetylacetone was sensitive to the moisture in air, during solid grinding process the relative humidity in air was required to be below 50%. If the relative humidity was high (such as 70% or above), catalysts prepared could not usually exhibit good performances.

2.4. Characterization of catalysts

Nitrogen adsorption-desorption isotherms at 77 K were recorded with a Micromeritics Tristar system. Before measurements, samples were outgassed at 473 K overnight. The BET surface area was calculated by applying the BET equation for relative pressure between 0.05 and 0.20. The pore size distribution was calculated from the adsorption branch by the Barret-Joyner-Halenda (BJH) method. HAADF-STEM (high-angle annular dark-field scanning transmission electron microscopy) observations were performed to observe tiny Au clusters on a JEOL JEM-3000F transmission electron microscope equipped with digitally processed STEM imaging system. Operating voltage was 300 kV and resolution was about 0.20 nm. The catalyst sample was directly dispersed on a micro-grid supported on a copper mesh without solvent. Elemental analysis was carried out by inductively coupled plasma-atomic emission spectroscopy (ICP-AES).

2.5. Catalytic tests

Propene epoxidation was carried out under atmospheric pressure. After the preparation of Au catalysts by solid grinding, 0.15 g of them was loaded into a vertical fixed-bed U-shaped quartz reactor with an inner diameter of 1.0 cm and then reduced by 10 vol% H_2 in Ar as described above. After the reduction Au catalysts were cooled down to room temperature in the same stream (H_2 , 10 vol%), and then feed gas containing C_3H_6 , O_2 , H_2 and Ar with volume ratio of 10/10/10/70 was passed through at a flow rate of 20 mL min^{-1} , which corresponded to a space velocity of $8000 \text{ mL g}_{\text{cat.}}^{-1} \text{ h}^{-1}$. Reaction temperature was raised from room temperature to 473 K with a heating rate of 1.0 K min^{-1} and then kept at 473 K. Reactants and products were analysed by on-line GCs equipped with TCD (Porapak Q column) and FID (HR-20 M column) detectors and auto-injector.

3. Results

3.1. Characterizations of supports

Fig. 1a shows the isotherms of TS-1(48) and alkaline treated TS-1(48) with NaOH aqueous solution. Over TS-1(48) the hysteresis loop, characteristic of mesopores, was absent, whereas over TS-1(48)-Na1 a small hysteresis loop can be observed, indicating the formation of small amount of mesopores. A larger

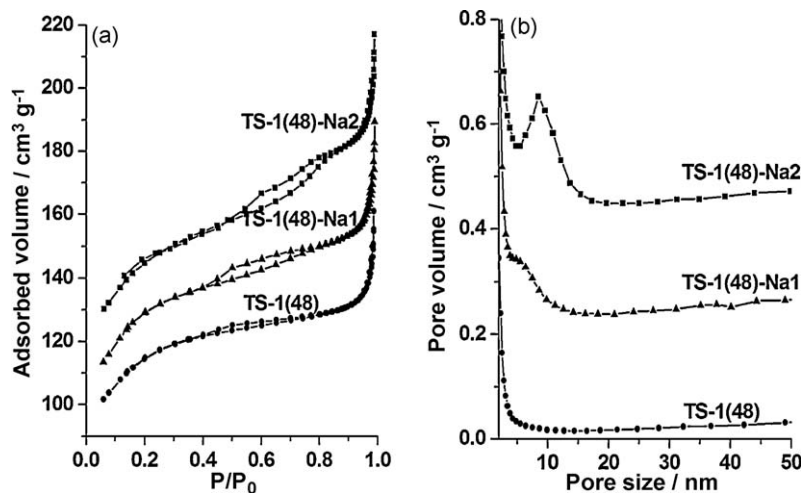


Fig. 1. N₂ adsorption–desorption isotherms (a) and pore size distributions (b) of TS-1(48), TS-1(48)-Na1, and TS-1(48)-Na2.

hysteresis loop at higher relative pressure can be clearly observed over TS-1(48)-Na2, indicating the enlargement of mesopores. The pore size distribution shown in Fig. 1b was in accordance with adsorption isotherms. Over TS-1(48)-Na1 some small mesopores were created with a shoulder peak of pore size at about 6.5 nm. Over TS-1(48)-Na2 well defined mesopores were created with a narrow pore size distribution centered at 8.6 nm. After alkaline treatment BET surface area (SA) and pore volume (PV) increased slightly (SA: 395, 397, 398 m² g⁻¹ and PV: 0.25, 0.27, 0.29 cm³ g⁻¹ over TS-1(48), TS-1(48)-Na1 and TS-1(48)-Na2, respectively).

Further characterizations of TS-1(48) with XRD, UV-vis spectroscopy and TEM (not shown) indicated that even after alkaline treatment crystalline MFI structure, coordination circumstance of Ti sites and shape of support particles were maintained. Similar phenomena were also observed after alkaline treatment of TS-1(88) and TS-1(36) with NaOH aqueous solution and TS-1(48) with LiOH, KOH, or CsOH aqueous solution.

Finally, elemental analyses were carried out for some representative supports and Au catalysts (Table 1). The content of Ti in TS-1(48) was 1.8 wt% (corresponding to a Si/Ti ratio of 43). In addition, 0.91 wt% of alkaline metal cations (K, 0.75 wt%; Na, 0.16 wt%) was detected, which should come from the impurities contained in tetrapropylammonium hydroxide (TPAOH) aqueous solution [24]. Alkaline treated TS-1(48), denoted as TS-1(48)-K1, contained the same amount of Ti of 1.8 wt%. Interestingly, K cation (0.95 wt%) was the only alkaline metal cation and Na cation was almost absent (<0.01 wt%). It is likely that similar phenomena might happen in TS-1(48)-Li1, TS-1(48)-Na1 and TS-1(48)-Cs1 and that Li, Na or Cs was the only alkaline metal cation, respectively. Total contents of alkaline metals would be maintained at the same level after alkaline treatment of TS-1 support.

3.2. Influence of alkaline treatment period of TS-1 support on the catalytic performance of Au catalysts

Fig. 2 and Table 2 shows the influence of alkaline treatment period on the catalytic performance of Au catalysts prepared by SG. Although high PO selectivity and high H₂ efficiency, 92% and 34%, respectively, were obtained with 0.10 wt% Au/TS-1(48), C₃H₆ conversion was very low (only 0.6%) resulting in a very low PO formation rate of 11 g_{PO} kg_{cat}⁻¹ h⁻¹. In contrast, with 0.10 wt% Au/TS-1(48)-Na1, C₃H₆ conversion was markedly enhanced to 7.4%, while high PO selectivity of 85% and high H₂ efficiency of 30% were maintained, leading to a high PO formation rate of 119 g_{PO} kg_{cat}⁻¹ h⁻¹. In addition, 0.10 wt% Au/TS-1(48)-Na1 could maintain high catalytic performance after catalytic test at 473 K for 15 h, C₃H₆ conversion of 7.2%, PO selectivity of 83%, and H₂ efficiency of 25%. The catalytic performance of 0.10 wt% Au/TS-1(48)-Na2 was inferior to that of 0.10 wt% Au/TS-1(48)-Na1, but superior to that of 0.10 wt% Au/TS-1(48). These results showed that pretreatment of TS-1(48) with aqueous NaOH solution before Au deposition can markedly improve the catalytic performance, in particular, PO formation rate. Similar phenomena were also observed over TS-1 with Si/Ti ratios other than 48 (Table 2). For example, 0.10 wt% Au/TS-1(88)-Na0.5 gave a PO formation ratio of 69 g_{PO} kg_{cat}⁻¹ h⁻¹, about 20 times higher than that (3.4 g_{PO} kg_{cat}⁻¹ h⁻¹) over 0.10 wt% Au/TS-1(88).

3.3. Influence of Au loadings on the catalytic performance of Au/alkaline treated TS-1

Since 0.10 wt% Au/TS-1(48)-Na1 presented the highest PO formation rate in Table 2, TS-1(48)-Na1 was chosen as a support to deposit Au by SG with different Au loadings of 0.05–0.50 wt%. The performance of these Au catalysts was shown in Fig. 3 and Table 3.

Table 1

Elemental and pore-structure analyses of typical supports and corresponding Au catalysts.

Supports and Au catalysts ^a	BET surface area (m ² g ⁻¹)	Mesopore size (nm)	Pore volume (cm ³ g ⁻¹)	Ti (wt%)	K (wt%)	Na (wt%)	Actual Au loading (wt%)	Mean Au diameter (nm) ^b
TS-1(48)	395	No	0.25	1.8	0.75	0.16	–	–
0.10 wt% Au/TS-1(48)	–	–	–	1.8	0.75	0.16	0.10	4.1
TS-1(48)-K1	400	6.8	0.28	1.8	0.95	<0.01	–	–
0.10 wt% Au/TS-1(48)-K1	–	–	–	1.8	0.95	<0.01	0.10	1.6

^a The wt% of Au denotes the calculated Au loadings and the figures in parentheses denote the calculated atomic ratios of Si/Ti for TS-1 synthesis.

^b The values were obtained by HAADF-STEM after epoxidation reaction for 15 h.

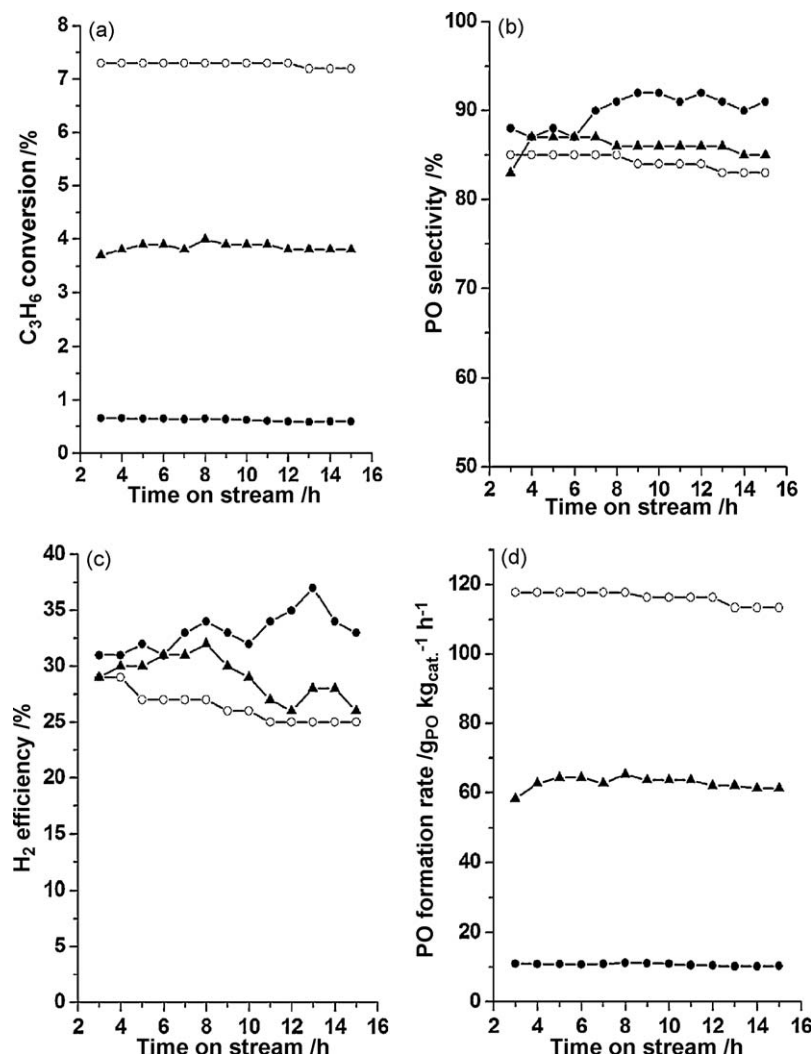


Fig. 2. Propene epoxidation with O₂ and H₂ mixture over Au deposited on TS-1(48) treated in alkaline solution for different periods. (a) C₃H₆ conversion; (b) PO selectivity; (c) H₂ efficiency; (d) PO formation rate (g_{PO} kg_{cat}⁻¹ h⁻¹). (●) 0.10 wt% Au/TS-1(48); (○) 0.10 wt% Au/TS-1(48)-Na1; (▲) 0.10 wt% Au/TS-1(48)-Na2. Reaction conditions: catalyst, 0.15 g; temperature, 473 K; feed gas, C₃H₆/O₂/H₂/Ar = 10/10/10/70 in vol%; space velocity, 8000 mL g_{cat}⁻¹ h⁻¹.

Although very high C₃H₆ conversion of 10% was obtained with 0.50 wt% Au/TS-1(48)-Na1, both PO selectivity and H₂ efficiency were very low, only 41% and 5.3%, respectively. For C₃H₆ epoxidation with O₂ and H₂ mixture, high PO selectivity can be achieved by controlling Au loading and by selecting reaction temperature: (1) high Au loading combined with low reaction temperature or (2) low Au loading combined with high reaction

temperature. Usually, the latter approach is better, because high reaction temperature facilitates PO desorption from the catalyst surfaces, resulting in longer lifetime of Au catalysts. Indeed, at 473 K over 0.25 wt% Au/TS-1(48)-Na1, PO selectivity was greatly improved to 82% with a high C₃H₆ conversion and a medium H₂ efficiency of 8.8% and 20%, respectively, leading to a high PO formation rate of 137 g_{PO} kg_{cat}⁻¹ h⁻¹, which was comparable to

Table 2

Propene epoxidation with O₂ and H₂ mixture over Au deposited on TS-1 treated with alkaline solution for different periods.

Au catalysts ^a	Conversion of C ₃ H ₆ (%)	Efficiency of H ₂ (%)	Selectivity (%)					PO formation rate (g _{PO} kg _{cat} ⁻¹ h ⁻¹)
			PO	PA	AC	EA	CO ₂	
Au/TS-1(36)	2.9	28	90	2.9	0.0	0.0	7.1	50
Au/TS-1(36)-Na1	3.3	26	86	2.6	0.8	1.2	9.2	54
Au/TS-1(36)-Na2	4.4	18	84	1.9	0.9	0.9	12.5	70
Au/TS-1(48)	0.6	34	92	0.0	0.0	0.0	7.8	11
Au/TS-1(48)-Na1	7.4	30	85	1.6	0.8	1.3	11.1	119
Au/TS-1(48)-Na2	3.8	31	87	2.3	0.7	0.9	9.2	63
Au/TS-1(88)	0.2	20	90	0.0	9.9	0.0	0.0	3.4
Au/TS-1(88)-Na0.5	4.2	19	87	1.6	0.6	0.9	9.8	69

Reaction conditions: feed gas, C₃H₆/O₂/H₂/Ar = 10/10/10/70 in vol%; space velocity, 8000 mL g_{cat}⁻¹ h⁻¹; temperature, 473 K. All the data were taken under a steady-state after 2.0 h duration. PO, propene epoxide; PA, propanal; AC, acetone; EA, ethanal.

^a Gold loading calculated from the quantity of dimethyl Au(III) acetylacetone used by the SG method was 0.10 wt%, and the figures in parentheses denote the atomic ratios of Si/Ti.

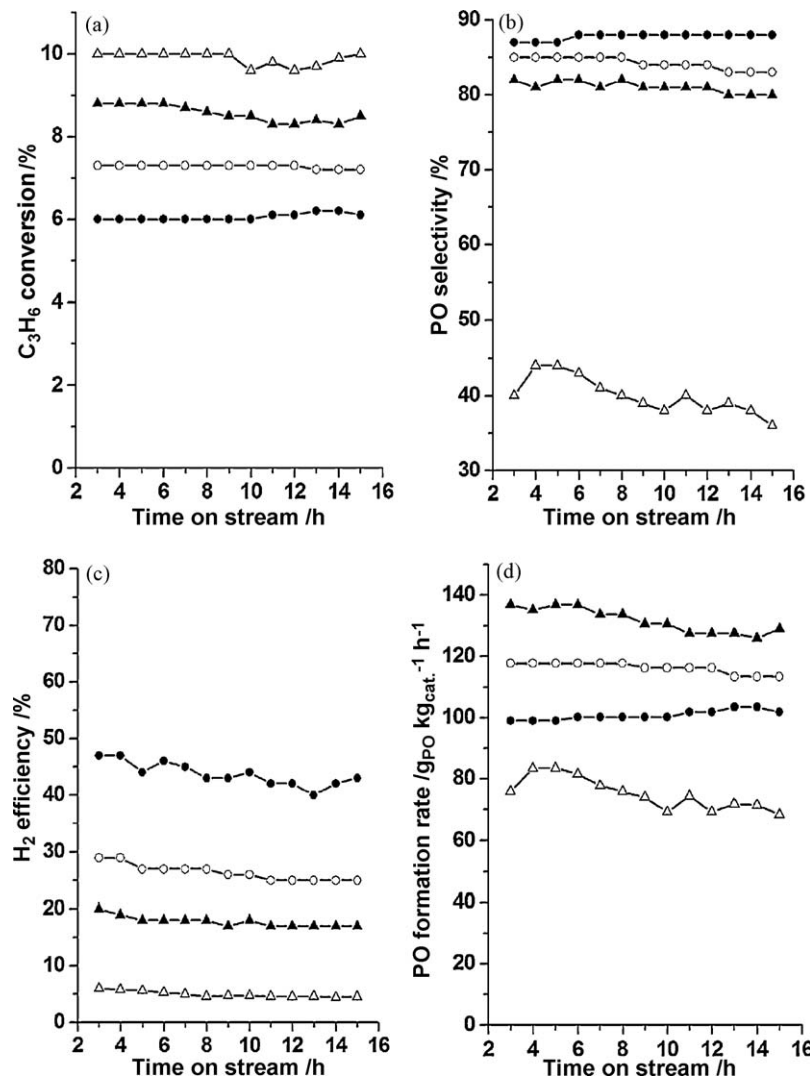


Fig. 3. Effect of Au loading (0.05–0.50 wt%) on the catalytic performance of Au/TS-1(48)-Na1 in C₃H₆ epoxidation with O₂ and H₂ mixture. (a) C₃H₆ conversion; (b) PO selectivity; (c) H₂ efficiency; (d) PO formation rate (g_{PO} kg_{cat.}⁻¹ h⁻¹). (●) 0.05 wt% Au/TS-1(48)-Na1; (○) 0.10 wt% Au/TS-1(48)-Na1; (▲) 0.25 wt% Au/TS-1(48)-Na1; (△) 0.50 wt% Au/TS-1(48)-Na1. Reaction conditions: catalyst, 0.15 g; temperature, 473 K; feed gas, C₃H₆/O₂/H₂/Ar = 10/10/10/70 in vol%; space velocity, 8000 mL g_{cat.}⁻¹ h⁻¹.

the best result (134 g_{PO} kg_{cat.}⁻¹ h⁻¹) reported by Delgass and co-workers [19,20].

Over Au/TS-1(48)-Na1 with a lower Au loading of 0.10 wt%, PO selectivity was further improved to 85%, while C₃H₆ conversion and PO formation rate decreased to 7.4% and 119 g_{PO} kg_{cat.}⁻¹ h⁻¹,

respectively. Interestingly, H₂ efficiency was appreciably raised to 30%. Hydrogen efficiency is an important parameter in the C₃H₆ epoxidation process with O₂ and H₂ mixture because it partly affects the economics of this process. Usually H₂ efficiency was low, less than 30%. The best H₂ efficiency reported so far is 35%,

Table 3

Propene epoxidation with O₂ and H₂ mixture over Au deposited on alkaline treated TS-1 with different Au loadings.

Au catalysts ^a	Conversion of C ₃ H ₆ (%)	Efficiency of H ₂ (%)	Selectivity (%)					PO formation rate (g _{PO} kg _{cat.} ⁻¹ h ⁻¹)
			PO	PA	AC	EA	CO ₂	
0.50 wt% Au/TS-1(48)-Na1 ^b	10	5.3	41	2.3	4.5	3.0	39	78
0.25 wt% Au/TS-1(48)-Na1	8.8	20	82	1.4	1.6	1.1	13	137
0.10 wt% Au/TS-1(48)-Na1	7.4	30	85	1.6	0.8	1.3	11	119
0.05 wt% Au/TS-1(48)-Na1	6.0	47	88	1.7	0.7	1.1	8.7	100
0.25 wt% Au/TS-1(48)-Li1	8.7	19	77	2.0	4.1	1.4	15	128
0.25 wt% Au/TS-1(48)-K1	9.7	7.0	53	0.9	0.5	1.2	44	98
0.10 wt% Au/TS-1(48)-K1	7.7	21	85	1.0	1.2	0.6	13	124
0.25 wt% Au/TS-1(48)-Cs1	8.4	12	74	0.4	0.7	0.9	24	118
0.10 wt% Au/TS-1(48)-Cs1	6.6	15	76	0.0	0.7	0.8	23	95

Reaction conditions: feed gas, C₃H₆/O₂/H₂/Ar = 10/10/10/70 in vol%; space velocity, 8000 mL g_{cat.}⁻¹ h⁻¹; temperature, 473 K. All the data were taken under a steady-state after 2.0 h duration. PO, propene epoxide; PA, propanal; AC, acetone; EA, ethanal.

^a Gold loadings were calculated from the quantity of dimethyl Au(III) acetylacetonate used by the SG method, and the figures in parentheses denote the atomic ratios of Si/Ti.

^b Over 0.50 wt% Au/TS-1(48)-Na1, acrolein was also produced with a selectivity of 11%.

which was achieved over barium-promoted Au/mesoporous Ti-SiO₂ in the presence of trimethylamine as a gas phase promoter [8]. Encouraged by the trend shown above that lower Au loadings resulted in higher H₂ efficiencies, Au was deposited on TS-1(48)-Na1 by SG with a low Au loading of only 0.05 wt%. Surprisingly, 0.05 wt% Au/TS-1(48)-Na1 initially presented a very high H₂ efficiency of 47%, better than any other reported one. More importantly, even after reaction at 473 K for 15 h H₂ efficiency was still as high as 43%. In addition, high C₃H₆ conversion of 6.0% and high PO selectivity of 88% were maintained, corresponding to a PO formation rate of about 100 g_{PO} kg_{cat.}⁻¹ h⁻¹.

3.4. Influence of different alkaline metal hydroxides on the catalytic performance of Au/alkaline treated TS-1

In order to know whether Au deposited on TS-1 pretreated in the aqueous solution of other alkaline metal hydroxides (LiOH,

KOH or CsOH) can also exhibit enhanced catalytic performance, TS-1(48)-Li1, TS-1(48)-K1 and TS-1(48)-Cs1 were selected to deposit 0.25 wt% and/or 0.10 wt% Au. As shown in Table 3, all these Au catalysts showed better catalytic performance than Au/TS-1(48) with PO formation rates between 95 g_{PO} kg_{cat.}⁻¹ h⁻¹ and 128 g_{PO} kg_{cat.}⁻¹ h⁻¹.

3.5. Influence of alkaline treatment of TS-1 support on the diameter distribution of Au particles

We used HAADF-STEM to obtain stronger contrasts for Au particles deposited on as prepared TS-1 and alkaline treated TS-1. In order to make more realistic information Au catalysts after reaction were observed. Low-magnification HAADF images showed that over 0.10 wt% Au/TS-1(48) only several large Au particles were present (Fig. 4a), while over 0.10 wt% Au/TS-1(48)-Na1 a plenty of small Au particles were almost uniformly dispersed

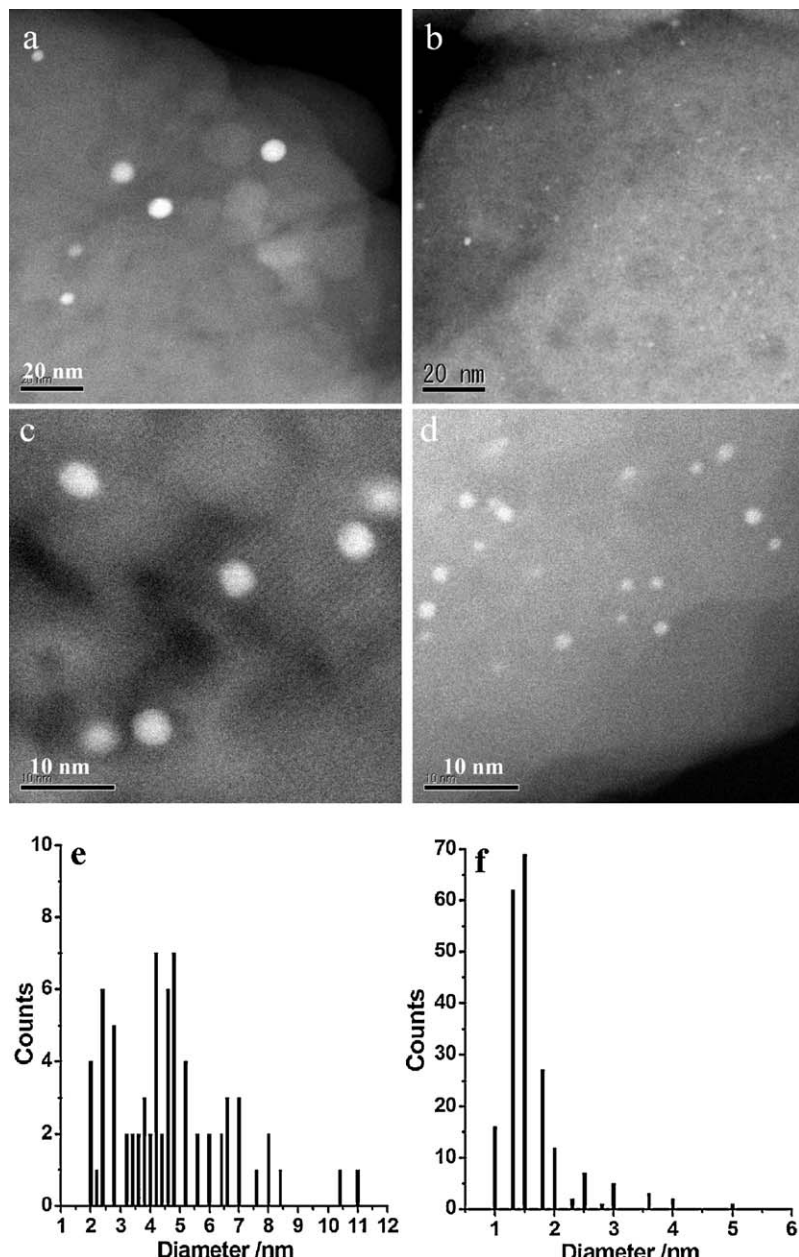


Fig. 4. HAADF-STEM images (a–d) and diameter distribution of Au particles (e and f) for 0.10 wt% Au/TS-1 (a, c and e) and 0.10 wt% Au/TS-1-Na1 (b, d and f). HAADF-STEM observation of Au catalysts was carried out after catalytic tests at 473 K for 15 h.

(Fig. 4b). In order to know the exact diameter of Au particles, high-magnification HAADF images were taken (Fig. 4c and d). Fig. 4c and e show that the diameter distribution of Au particles for 0.10 wt% Au/TS-1(48) was very broad (2.0–11 nm), giving a mean Au diameter of 4.1 nm. In contrast, in 0.10 wt% Au/TS-1(48)-Na1 only minor fraction (about 10%) of Au particles existed as nanoparticles (NPs) larger than 2.0 nm, and about 90% of Au particles existed as clusters with diameters in the range of 1.0–2.0 nm (Fig. 4d and f). The size distribution (Fig. 4f) suggested that about 65% of Au particles existed as Au_{55} clusters with diameters in the range of 1.3–1.6 nm [25]. Similar diameter distribution of Au particles was also observed for 0.10 wt% Au/TS-1(48)-K1 and other Au/alkaline treated TS-1(48) (not shown). It was very difficult to find Au clusters smaller than 1.0 nm (detection limit of HAADF-STEM: 0.6 nm), however, even if Au clusters in the diameter range of 0.6–1.0 nm were formed in 0.10 wt% Au/TS-1(48) and in 0.10 wt% Au/TS-1(48)-Na1, their quantity is very small.

4. Discussion

4.1. The role of alkaline treatment of TS-1 support

Concerning the reasons why Au clusters could be stabilized by alkaline treated TS-1, as shown in Scheme 1, during SG process organic Au species were mostly deposited on the exterior surfaces of as prepared TS-1 and alkaline treated TS-1. It was experimentally not easy to incorporate Au species into the MFI micropores by SG. This point of view was approved by the fact that during solid grinding dimethyl Au(III)acetylacetone with mesoporous supports (such as Ti-MCM-41), Au species were selectively deposited on the exterior surfaces of mesoporous materials as nanoparitcles (>2.0 nm), and it was very difficult to distinguish whether Au clusters or nanoparticles were incorporated into mesopores or not by TEM characterization. Over the smooth exterior surfaces of as prepared TS-1, organic Au complexes (most likely dimethyl Au(III) ligands) are adsorbed and partly reduced, and then Au clusters (<2.0 nm) aggregates to form Au NPs (>2.0 nm) during SG, which was confirmed by the color change from white to pink. After reduction by H_2 at 423 K and catalytic test at 473 K, only Au NPs could be observed over Au/TS-1 by HAADF-STEM (Fig. 4a and c) and the pink color was intensified. In contrast, over the rough exterior surfaces of alkaline treated TS-1, owing to the presence of large amount of defects and small mesopores, where organic Au species can be strongly fixed, the resulting Au clusters (<2.0 nm) are mostly confined to the surfaces and do not coagulate to form Au NPs (>2.0 nm) during SG, reduction by H_2 , and catalytic tests. Similar phenomenon was also observed that the rough surfaces of TiO_2 can stabilize Au NPs during CO oxidation [26]. Based on the results above, a simple but effective way to prepare stable Au clusters could be proposed: roughening the surfaces of supports before Au deposition to increase the amount of surface defects.

4.2. Improved catalytic performance of Au/alkaline treated TS-1

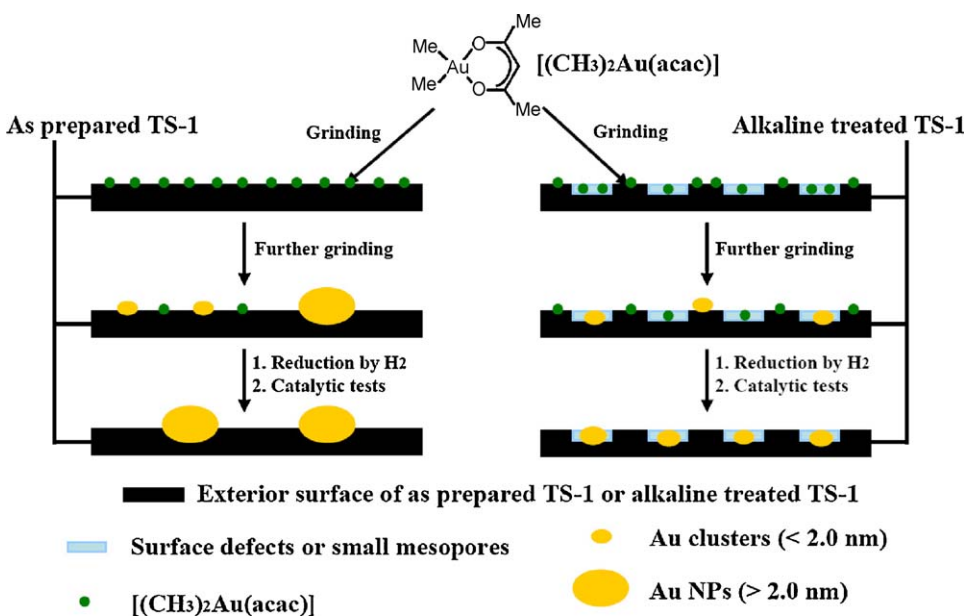
As for PO synthesis by C_3H_6 epoxidation with O_2 and H_2 mixture over Au catalysts, the size of Au particles is very important. Over Au/TiO_2 catalyst Au NPs with diameter of 2.0–5.0 nm are responsible for PO synthesis, while Au NPs larger than 5.0 nm cause complete combustion of C_3H_6 to CO_2 and Au clusters smaller than 2.0 nm result in the hydrogenation of C_3H_6 to propane (C_3H_8). As for Au/TS-1 catalysts, Delgass and co-workers assumed that tiny Au clusters smaller than 1.0 nm (4 atoms or 7 atoms Au clusters) might be responsible for PO synthesis [17], although these tiny clusters were invisible by TEM due to the weak contrast against the background of TS-1 support. EXAFS characterization of Au catalysts active for C_3H_6 epoxidation with O_2 and H_2 mixture indicated the

presence of larger Au clusters (0.9–2.0 nm) [10,14]. Here, our HAADF-STEM characterization directly confirmed the presence of a large number of Au clusters smaller than 2.0 nm but larger than 1.0 nm over the exterior surface of Au/alkaline treated TS-1. These relatively large Au clusters (1.0–2.0 nm), most likely Au_{55} clusters (1.3–1.6 nm), can explain the improved catalytic performance of Au/alkaline treated TS-1, such as PO formation rate and H_2 utilization efficiency.

Although Au/alkaline treated TS-1 exhibited greatly enhanced PO formation rate in comparison to Au/TS-1, as prepared TS-1 and alkaline treated TS-1 possessed similar BET surface area, coordination circumstance of Ti sites, crystalline MFI structure, shape of support particles and contents of alkaline metals. In addition, Au/TS-1 and Au/alkaline treated TS-1 such as 0.10 wt% Au/TS-1(48) and 0.10 wt% Au/TS-1(48)-K1, respectively, possessed the same Au loading and the same Ti content (Table 1). Therefore, the greatly enhanced PO formation rate over Au/alkaline treated TS-1 can be ascribed to the presence of Au clusters (<2.0 nm), which is in accordance with the statement by Oyama and co-workers based on EXAFS analyses [10]. This interpretation was approved by the fact that Au NPs (>2.0 nm) deposited on Ti-MCM-41 and Ti-TUD-1 by solid grinding can only display the low catalytic performance with C_3H_6 conversion less than 2.0% and PO selectivity less than 80%. Interestingly, with the diameter decrease of Au particles from 4.1 nm [over 0.10 wt% Au/TS-1(48)] to 1.6 nm [over 0.10 wt% Au/TS-1(48)-K1], the molar ratio of active surface Au atoms (exposed to reactant feed gas) to total Au atoms will increase only about 3 times, while 0.10 wt% Au/TS-1(48)-K1 exhibited a high PO formation rate of $124 \text{ g}_{\text{PO}} \text{ kg}_{\text{cat}}^{-1} \text{ h}^{-1}$, 10 times higher than that of $11 \text{ g}_{\text{PO}} \text{ kg}_{\text{cat}}^{-1} \text{ h}^{-1}$ over 0.10 wt% Au/TS-1(48). The catalytic performance per surface Au atoms in 0.10 wt% Au/TS-1(48)-K1 was about 2.7 times higher than that in 0.10 wt% Au/TS-1.

In our present work very high H_2 efficiency of 47% was achieved over 0.05 wt% Au/TS-1(48)-Na1 even in the absence of any promoters (Fig. 3 and Table 3), better than the highest H_2 efficiency of 35% reported so far [8]. Oyama and co-workers has observed that in Au/mesoporous Ti-SiO_2 catalysts small Au clusters (0.9 nm, from EXAFS) displayed much higher H_2 efficiency in C_3H_6 epoxidation with O_2 and H_2 than larger Au clusters (2.0 nm from TEM or 1.4 nm from EXAFS) [10]. Therefore, in our work HAADF-STEM was used to observe the influence of Au loading on the diameter of Au clusters in 0.10 wt% Au/TS-1(48)-K1 and 0.20 wt% Au/TS-1(48)-K1. It was found that even if Au loading was doubled from 0.10 wt% to 0.20 wt%, the mean diameter of Au clusters only slightly increased from 1.6 nm (Table 1) to 1.8 nm [27], and the molar ratios of Au clusters (1.3–1.6 nm, most likely 55 atoms) to total Au particles in both catalysts were almost the same (about 65%). It might be reasonably assumed that in 0.05 wt% Au/TS-1(48)-Na1 and 0.25 wt% Au/TS-1(48)-Na1, Au_{55} clusters would be the majority of Au particles, similar to the case of 0.10 wt% Au/TS-1(48)-Na1 (Fig. 4f). Therefore, the very different H_2 efficiency of 47%, 30% and 20% over these three Au catalysts (Table 3) might be caused not by the different diameter of Au clusters but by the very different ratios of Au_{55} clusters to isolated Ti^{4+} sites.

In our work, as prepared TS-1 and alkaline treated TS-1 particles possessed the diameters of about 170 nm, and herein isolated Ti sites on the exterior surfaces were estimated to be about 2.1% of total Ti content [17]. In Au/TS-1(48)-Na1 with Au loading of 0.05 wt%, 0.10 wt% and 0.25 wt% the ratio of Au atoms (if exclusively deposited on the exterior surfaces) to exterior isolated Ti^{4+} sites was about 0.32, 0.64 and 1.61, and thus the ratios of Au_{55}/Ti were 0.58%, 1.2% and 2.9%, respectively (supposing all the Au atoms aggregate to form only Au_{55} clusters). It appeared that lower ratio of Au_{55}/Ti in Au/alkaline treated TS-1 favored higher H_2 efficiency. This hypothesis has been confirmed by the following examples. Although Au_{55} clusters (1.6 nm) in 0.10 wt% Au/TS-1(48)-Na1 should give a much



Scheme 1. Possible pathways for the formation of Au NPs or clusters by solid grinding of $[(CH_3)_2Au(acac)]$ with TS-1 or alkaline treated TS-1.

higher H_2 efficiency than Au NPs (4.1 nm) in 0.10 wt% Au/TS-1(48) [10]. Table 2 showed that 4.1-nm Au NPs presented slightly higher H_2 efficiency than 1.6-nm Au_{55} clusters (34% and 30%, respectively). The phenomena that lower density of active Au particles favors higher H_2 efficiency might be explained as follows. Firstly, O_2 reacts with H_2 over the surface of Au particles to produce H_2O_2 , and then synthesized H_2O_2 transfers from Au surface to bare Ti sites to form $Ti-OOH$, which is active for PO synthesis. The effective capture of H_2O_2 by bare Ti sites to form $Ti-OOH$ becomes very important for C_3H_6 epoxidation, otherwise, H_2O_2 will directly decompose to produce H_2O and not contribute to PO synthesis. It is reasonable that larger amount of bare Ti sites near Au particles, at the cost of lower density of Au particles, will lead to higher capture efficiency of H_2O_2 , and thus higher H_2 utilization efficiency. This fact above suggested that the ratio of Au particles (clusters or NPs) to isolated Ti^{4+} sites played a more important role in influencing H_2 efficiency than the size of Au particles.

4.3. Improved catalytic stability

In C_3H_6 epoxidation with O_2 and H_2 Au/TS-1 exhibited better catalytic stability than Au/TiO₂ and Au/mesoporous Ti-SiO₂ [6,7,12,13,17,18], while related explanations were absent. In our experiments highly active Au/alkaline treated TS-1 also displayed excellent stability during testing period of 15 h (Figs. 2 and 3). Since at a reaction temperature as high as 473 K PO can be easily desorbed from the surface of catalysts, the catalytic stability of Au/alkaline treated TS-1 may come from the stability of Au clusters. Although the exact diameter distribution of Au particles over fresh Au/alkaline treated TS-1 (before reaction) was not obtained, after reaction at 473 K for 15 h, as shown in Fig. 4 most (about 90%) of Au particles in 0.10 wt% Au/TS-1(48)-Na1 could still exist as clusters (1.0–2.0 nm), giving a mean diameter of 1.6 nm. Recent work showed that Au clusters ($< 2.0\text{ nm}$) supported on alkaline treated TS-1 [27] and tiny Au_{7-10} clusters supported on amorphous Al₂O₃ [28] could catalyze C_3H_6 epoxidation with O_2 and H_2O mixture. Gold clusters ($< 2.0\text{ nm}$) on 0.20 wt% Au/TS-1(48)-K1 were very stable, giving a mean diameter of Au clusters of 1.6 nm (before reaction) and 1.8 nm (after reaction at 473 K for 21 h) [27]. More surprisingly, even after calcining at 573 K and subsequent reaction at 473 K for 21 h, a mean diameter of 2.0 nm can be still kept over

this Au catalyst. Therefore, it is very likely that the excellent stability of Au clusters supported on alkaline treated TS-1 against coagulation leads to excellent catalytic stability of Au/alkaline treated TS-1 in C_3H_6 epoxidation with O_2 and H_2 .

5. Conclusions

- (1) Solid grinding (SG) method using dimethyl Au(III) acetylacetone can deposit Au on as prepared TS-1 and alkaline treated TS-1 with a very high Au capture efficiency of about 100%, which is much higher than the efficiency (<20%) by deposition-precipitation method using HAuCl₄ and NaOH.
- (2) Pretreatment of TS-1 supports with aqueous alkaline metal hydroxides before Au deposition is crucial to prepare Au clusters smaller than 2.0 nm by SG and thus to achieve high catalytic performance. In contrast, over as prepared TS-1, only Au nanoparticles (NPs) larger than 2.0 nm are formed.
- (3) The turnover frequency for propene epoxidation based on surface exposed Au atoms of gold clusters with a mean diameter of 1.6 nm was about 2.7 times higher than that of Au NPs with a mean diameter of 4.1 nm.
- (4) The balance and/or configuration between Au clusters and isolated Ti^{4+} sites appears to be very important to both PO formation rate and H_2 efficiency. Low ratios of Au clusters to isolated Ti^{4+} sites (such as in 0.05 wt% Au/TS-1(48)-Na1) lead to a H_2 efficiency as high as 47% but a relatively low PO formation rate, while high ratios of Au clusters to isolated Ti^{4+} sites (such as in 0.25 wt% Au/TS-1(48)-Na1) lead to relatively low H_2 efficiency but high PO formation rate (as high as $137\text{ g}_{PO}\text{ kg}_{cat}^{-1}\text{ h}^{-1}$). The optimum Au loading for overall catalytic performance is 0.05 wt% or 0.10 wt% at Si/Ti of 48.

Acknowledgement

We are grateful to Dr. Tamao Ishida for her critical discussion about sample characterization by TEM.

References

- [1] F. Nees, Heterogeneous catalysis at BASF (available at <http://basf.com/group/corporate/en/innovations/events-presentations/catalysis/papers>), 2008.

- [2] S.T. Oyama, Mechanism in Homogeneous and Heterogeneous Epoxidation Catalysis, Elsevier B.V., Amsterdam, 2008.
- [3] M. Ishino, J. Yamamoto, Shokubai (Catalysts & Catalysis) 48 (2006) 511.
- [4] A.H. Tullo, P.L. Short, Chem. Eng. News 84 (41) (2006) 22.
- [5] J.M. Campos-Martin, G. Blanco-Brieva, J.L.G. Fierro, Angew. Chem. Int. Ed. 45 (2006) 6962.
- [6] T. Hayashi, K. Tanaka, M. Haruta, J. Catal. 178 (1998) 566.
- [7] A.K. Sinha, S. Seelan, S. Tsubota, M. Haruta, Angew. Chem. Int. Ed. 43 (2004) 1546.
- [8] B. Chowdhury, J.J. Bravo-Suárez, M. Daté, S. Tsubota, M. Haruta, Angew. Chem. Int. Ed. 45 (2006) 412.
- [9] B. Chowdhury, J.J. Bravo-Suárez, N. Mimura, J. Lu, K.K. Bando, S. Tsubota, M. Haruta, J. Phys. Chem. B 110 (2006) 22995.
- [10] J. Lu, X. Zhang, J.J. Bravo-Suárez, K.K. Bando, T. Fujitani, S.T. Oyama, J. Catal. 250 (2007) 350.
- [11] J.J. Bravo-Suárez, K.K. Bando, J. Lu, M. Haruta, T. Fujitani, S.T. Oyama, J. Phys. Chem. C 112 (2008) 1115.
- [12] S.T. Oyama, X. Zhang, J. Lu, Y. Gu, T. Fujitani, J. Catal. 257 (2008) 1.
- [13] T.A. Nijhuis, T. Visser, B.M. Weckhuysen, Angew. Chem. Int. Ed. 44 (2005) 1115.
- [14] E. Sacaliciuc, A.M. Beale, B.M. Weckhuysen, T.A. Nijhuis, J. Catal. 248 (2007) 235.
- [15] T.A. Nijhuis, M. Makkee, J.A. Moulijn, B.M. Weckhuysen, Ind. Eng. Chem. Res. 45 (2006) 3447.
- [16] A. Zwijnenburg, M. Makkee, J.A. Moulijn, Appl. Catal. A 270 (2004) 49.
- [17] N. Yap, R.P. Andres, W.N. Delgass, J. Catal. 226 (2004) 156.
- [18] B. Taylor, J. Lauterbach, W.N. Delgass, Appl. Catal. A 291 (2005) 188.
- [19] L. Cumaranatunge, W.N. Delgass, J. Catal. 232 (2005) 38.
- [20] B. Taylor, J. Lauterbach, W.N. Delgass, Catal. Today 123 (2007) 50.
- [21] J. Lu, X. Zhang, J.J. Bravo-Suárez, T. Fujitani, S.T. Oyama, Catal. Today 147 (2009) 186.
- [22] M. Ishida, M. Nagaoka, T. Akita, M. Haruta, Chem. Eur. J. 14 (2008) 8456.
- [23] M. Ishida, N. Kinoshita, H. Okatsu, T. Akita, T. Takei, M. Haruta, Angew. Chem. Int. Ed. 47 (2008) 9265.
- [24] T. Tatsumi, K.A. Koyano, Y. Shimizu, Appl. Catal. A 200 (2000) 125.
- [25] M. Turner, V.B. Golovko, O.P.H. Vaughan, P. Abdulkin, A. Berenguer-Murcia, M.S. Tikhov, B.F.G. Johnson, R.M. Lambert, Nature 454 (2008) 981.
- [26] M. Valden, X. Lai, D.W. Goodman, Science 281 (1998) 1647.
- [27] J. Huang, T. Akita, J. Faye, T. Fujitani, T. Takei, M. Haruta, Angew. Chem. Int. Ed. 48 (2009) 7862.
- [28] S. Lee, L.M. Molina, M. López, J.A. Alonso, B. Hammer, B. Lee, S. Seifert, R.E. Winans, J.W. Elam, M.J. Pellin, S. Vajda, Angew. Chem. Int. Ed. 48 (2009) 1467.